

Accepted Manuscript

Magnetic and magneto-optical properties of films of multiferroic GdMnO₃ grown on LSAT [(LaAlO₃)_{0.3} (Sr₂AlTaO₆)_{0.7}] (100) and (111)

Hasan Albargi, Mohammed Alqahtani, H.J. Blythe, A.M. Fox, N. Andreev, V. Chichkov, G.A. Gehring



PII: S0040-6090(17)30819-2
DOI: doi:[10.1016/j.tsf.2017.10.057](https://doi.org/10.1016/j.tsf.2017.10.057)
Reference: TSF 36325

To appear in: *Thin Solid Films*

Received date: 14 December 2016

Revised date: 5 October 2017

Accepted date: 28 October 2017

Please cite this article as: Hasan Albargi, Mohammed Alqahtani, H.J. Blythe, A.M. Fox, N. Andreev, V. Chichkov, G.A. Gehring, Magnetic and magneto-optical properties of films of multiferroic GdMnO₃ grown on LSAT [(LaAlO₃)_{0.3} (Sr₂AlTaO₆)_{0.7}] (100) and (111). The address for the corresponding author was captured as affiliation for all authors. Please check if appropriate. Tsf(2017), doi:[10.1016/j.tsf.2017.10.057](https://doi.org/10.1016/j.tsf.2017.10.057)

This is a PDF file of an unedited manuscript that has been accepted for publication. As a service to our customers we are providing this early version of the manuscript. The manuscript will undergo copyediting, typesetting, and review of the resulting proof before it is published in its final form. Please note that during the production process errors may be discovered which could affect the content, and all legal disclaimers that apply to the journal pertain.

Magnetic and Magneto-optical properties of films of multiferroic GdMnO₃ grown on LSAT [(LaAlO₃)_{0.3} (Sr₂AlTaO₆)_{0.7}] (100) and (111)

Hasan Albargi^{1,2}, Mohammed Alqahtani^{1,3}, H.J Blythe¹, A.M. Fox¹, N. Andreev⁴, V. Chichkov⁴, and
G.A. Gehring¹

Final version

¹*Department of Physics and Astronomy, University of Sheffield, Sheffield S3 7RH, UK*

²*Department of Physics, Najran University, P.O. Box: 1988, Najran 11001, Saudi Arabia*

³*Department of Physics and Astronomy, King Saud University, P.O. Box 2455, Riyadh 11451, Saudi Arabia*

⁴*National University of Science and Technology "MISiS", Leninskii Prospect 4, 119049 Moscow. Russia*

Abstract

The magnetic properties of multiferroic GdMnO₃ depend on strain which is produced in a thin film by growing an epitaxial film on a suitable substrate. We report an investigation of the magnetic and optical properties of GdMnO₃, as a function of strain, produced by growing epitaxial films on the substrates on (LaAlO₃)_{0.3}(Sr₂AlTaO₆)_{0.7} (LSAT) (100) and (111). Magnetic measurements have shown that at 5K the easy direction of the film is in-plane for LSAT (100) and the canted moment is significantly smaller than the value found in bulk material but larger than that found for GdMnO₃ on SrTiO₃ (100). The coercive field of the GdMnO₃/LSAT (100) has also been found to be smaller than for bulk single crystal samples but comparable to a thinner film of GdMnO₃ grown on SrTiO₃. The magnetic properties of the film grown on LSAT (111) are very different. The transition to the canted phase is less pronounced and there is no magnetic hysteresis at low temperatures. The susceptibility data are fitted with the Curie's law and the measured magnetic moments for the film on LSAT (100) were similar to bulk values but significantly different for films on LSAT (111) and SrTiO₃

(100). The magnetic circular dichroism spectroscopy showed two features: the charge transfer transition between Mn d states at ~ 2 eV and the band edge transition from the oxygen p band to the d states at ~ 3 eV. Magnetic circular dichroism also shows that the transition at around 2 eV is stronger in LSAT (100) than in LSAT (111) implying that the structure of the film of GdMnO_3 is closer to that of LaMnO_3 when grown on LSAT (100).

I. INTRODUCTION

Multiferroic rare-earth materials exhibit ferroelectric and magnetic ordering simultaneously and have received a large amount of interest due to the potential of exploiting them in spintronic applications. Investigations of the multiferroic materials started in the 1960's [1-5]. However, since 2001 the research in this field has received much interest because these materials have been found to have complicated magnetic states at low temperature and also multiferroic properties [2, 6, 7]. The magnetic interactions can be calculated depending on the orbital overlap of electrons, using the Goodenough-Kanamori rules [6, 8-10]. The manganites can be divided into two groups: a hexagonal phase ($P6_3cm$) with R (= Ho, Er, Tm, Yb, Y and Lu) which have smaller ionic radii and an orthorhombic phase ($Pnma$) with R (= La, Pr, Nd, Sm, Eu, Gd, Tb and Dy) which have larger ionic radii [6, 10, 11]. The boundary between these two groups is between DyMnO_3 and HoMnO_3 . For those compounds that are located close to the boundary in the orthorhombic phase, such as DyMnO_3 and TbMnO_3 , structural phase transitions occur which have caused them to be studied extensively.

GdMnO_3 (GMO) is an interesting multiferroic candidate; it has an orthorhombic distorted perovskite lattice structure with lattice parameters $a = 5.310 \text{ \AA}$, $b = 5.840 \text{ \AA}$, $c = 7.430 \text{ \AA}$. This is formed from the cubic phase by a rotation of the oxygen octahedra in which the a and b axes are rotated by $\pi/4$ from the original cubic, x , y axes and the c axis is doubled. Magnetic frustration is attributed to

competing exchange integrals between alternating neighbours that maintain the spiral magnetic phase below the Néel temperature T_N [12, 13].

GMO contains Gd^{3+} which has a large spin moment, $S = 7/2$ and $g = 2$, and hence a large value of $g[S(S+1)]^{1/2}$ as well as Mn^{3+} , $S = 2$, where the highest occupied d state is the singly occupied e_g orbital that is split by a Jahn-Teller interaction. The ionic radius of Gd^{3+} is located in the region between La and Dy ; this causes its physical properties to be a sensitive function of strain. Bulk crystalline GMO undergoes a phase transition to an incommensurate antiferromagnetic phase at ~ 42 K and to a canted antiferromagnetic phase at ~ 23 K. A ferroelectric phase is induced at ~ 6.5 K by applying a magnetic field along the b axis; the phase boundaries depend on both the magnitude and direction of the magnetic field [14-16]. The exchange interaction between the Mn ions is very sensitive to strain, which is why there is a coupling between the spin structure and the ferroelectricity. GMO has a strong optical transition at ~ 3.5 eV and a weaker $d-d$ transition at ~ 2 eV, which involves a transition between the components of the Jahn–Teller doublet and hence is strongly dependent on an applied magnetic field [15]. This transition gives rise to a clear signal in magnetic circular dichroism (MCD)[4].

An earlier study of GMO grown on $SrTiO_3$ (STO) was limited by two factors [4]: firstly there is strong absorption from STO above 3.2 eV thus preventing any optical studies above this energy, and secondly STO has a structural phase transition at around 110 K which further strains the film but also provides birefringence, which makes magneto-optic measurements very difficult. Both of these disadvantages are mitigated for $(LaAlO_3)_{0.3}(Sr_2AlTaO_6)_{0.7}$, (LSAT), which has an energy gap at 4.9 eV [17], hence the absorption in the range $1.5 < E < 4.5$ eV is much less than for STO and there is no structural transition. LSAT is cubic but with a slightly smaller lattice constant, 3.868 Å, than $SrTiO_3$, 3.905 Å.

In this work epitaxial films of grown on LSAT(100) and (111) have been investigated and compared with earlier work of GMO on $SrTiO_3$ (100) [4]. The different strains and orientation of the films on these two substrates give rise to novel effects.

II. EXPERIMENTAL PROCEDURE

The GMO films were grown using RF microwave sputtering from Gd_2O_3 and MnO_2 targets on LSAT (100) and (111) substrates. The films, of thickness 100nm, were grown in a mixture of Ar and O_2 pressure of 0.133 – 0.267 Pa and the substrate temperature was fixed at 650°C. The structures of the films have been analyzed by x-ray diffraction (XRD) and found to be epitaxial on LSAT (100) and (111) substrates. The magnetic properties of the films have been studied at room temperature and low temperature, 5 K, using a SQUID magnetometer, to measure the hysteresis loops. The field cooled/zero field cooled (FC/ZFC) magnetisation measurements were made by continuously measuring the magnetisation while cooling the sample to 5K in the presence of an, in-plane, magnetic field of $8 \times 10^{-3} \text{Am}^{-1}$, and then warming up to room temperature in the same field. Hysteresis loops were measured at 300K and 5K with the magnetic field applied both in-plane and out-of-plane of the films. The absorption data have been deduced from the transmission and reflection measurements, which were made at room temperature. The films have been studied using magneto-optic spectroscopy in Faraday geometry at room temperature and at 10 K using a Xenon lamp and a monochromator over the energy range 1.5 eV – 3.8 eV [4].

III. PROPERTIES OF LSAT

LSAT has been used widely as a substrate because it grows as an untwinned cubic perovskite with lattice parameter $a_0 = 3.868 \text{ \AA}$ which is an excellent lattice match to both cuprate superconductors and the colossal resistive manganites. Our substrates were obtained from MTI Corp; both (100) and (111) substrates had thicknesses of 0.5 mm ± 0.05 mm and were oriented to within $\pm 0.5^\circ$; they were polished on both sides and had surface roughness $R_a < 8 \text{ \AA}$. No twinning or domains were detected by MTI Corp, or in our XRD analysis. In this study we need to investigate the optical and magnetic properties of LSAT so that these effects can be subtracted from our measurements of GMO on these substrates.

LSAT is a substitutionally disordered oxide containing divalent Sr, trivalent La and Al and pentavalent Ta and hence has much local disorder. The measured transmission, T , at 2eV is ~ 0.8 which is comparable with the value expected from a smooth transparent substrate, $T = \frac{2n}{n^2 + 1} = 0.79$ at 2eV using the refractive index of LSAT, which is 2.02 at 2 eV [12, 18]. The transmission at 4.5eV $\sim 40\%$ is considerably less than that for a transparent substrate $T = 0.74$ ($n = 2.24$) indicating that the LSAT is absorbing above 3.7eV as shown in Fig.1(a) [17]. These transitions are very weak since the transmission was measured on a substrate of thickness 0.5mm. There is no difference between T measured for the two orientations. The absorption of the GMO can be seen from Fig 1(b) from the difference between Figs 1(a) and (b), this is discussed in Section VI.

Many disordered oxides have small magnetic moments, hence we needed to measure the magnetic properties of the substrates carefully, so that the results for magnetisation of the films on the substrates could be found [19]. The expected diamagnetic contribution dominates in the FC/ZFC magnetisation at high temperatures, $M \sim -1.7 \times 10^{-9} \text{ Am}^2$ in a field of $8 \times 10^{-3} \text{ Am}^{-1}$ and is the same for both substrates in each orientation. There is a paramagnetic contribution as shown in Figs 2(a) which was not visible at room temperature.

We postulate that the paramagnetic response is from the electrons in the localised states that gave rise to the observed absorption for energies greater than 3.5eV.

Hysteresis loops for LSAT (100) and LSAT (111), were measured at 5 K and 300 K with a magnetic field applied in parallel and perpendicular directions, and show very small coercive fields when taken at 5 K with the field in plane as shown in Figs. 2 (e) and (f). This must be due to a small contamination. These effects set the limit of what values can be measured reliably for the films [16, 19]. All the magnetic results presented for the GMO films in Sections V and VII have been corrected for the contributions of the LSAT.

IV. STRUCTURE OF GMO ON LSAT

The structure was investigated by x-ray diffraction. The lattice constant of LSAT is $a_0 = 3.868 \text{ \AA}$ compared with those for GMO: $a = 5.310 \text{ \AA}$, $b = 5.840 \text{ \AA}$ and $c = 7.430 \text{ \AA}$. Detailed measurements were made for the film on LSAT (100) using $\text{CoK}\alpha$ radiation and the results shown in Fig. 3. The results are indexed using $P6mm$ [20].

For the (100) substrate we found that there were two dominant orientations, (a) $(110)_{\text{GMO}} \parallel (100)_{\text{LSAT}}$; $[001]_{\text{GMO}} \parallel [010]_{\text{LSAT}}$ and (b) $(110)_{\text{GMO}} \parallel (100)_{\text{LSAT}}$, $[001]_{\text{GMO}} \parallel [001]_{\text{LSAT}}$. Two other orientations occurring less frequently were (c) $(001)_{\text{GMO}} \parallel (100)_{\text{LSAT}}$, $[010]_{\text{GMO}} \parallel [010]_{\text{LSAT}}$ and (d) $(001)_{\text{GMO}} \parallel (100)_{\text{LSAT}}$, $[100]_{\text{GMO}} \parallel [010]_{\text{LSAT}}$. In structures (a) and (b) the separation of the (110) planes

$$d_{110}^{\text{GMO}} = \left[\left(\frac{1}{a} \right)^2 + \left(\frac{1}{b} \right)^2 \right]^{-1/2} = 3.93 \text{ \AA} \text{ this needs a small contraction, 1.5\% to fit } d_{100}^{\text{LSAT}} = 3.868 \text{ \AA}. \text{ There}$$

is an expansion of 4% and a smaller contraction 2% that occur in plane as the GMO $[001]$ and $[1\bar{1}0]$ axes respectively fit to LSAT $[020]$ or $[002]$ as given in Table I. For cases (c) and (d) the misfit between the planes GMO (001) and LSAT (100) forces an expansion of 4% along $[001]$ ($d_{001}^{\text{GMO}} = 7.430 \text{ \AA}$ and $2 d_{100}^{\text{LSAT}} = 7.736 \text{ \AA}$) and there are also contractions in the two in-plane lattice vectors GMO $[100]$ and $[010]$. Thus the majority of the film has the plane aligned with the least strains. The results are summarized in the following Table I.

The XRD results for the LSAT (111) and $\text{GdMnO}_3/\text{LSAT}$ (111) samples are shown in Fig. 4. On the LSAT (111) substrate, the highest peaks correspond to the GMO(202) and GMO(022) planes. The

separations of the (202) and (022) planes are given by $\frac{1}{2} \left[\left(\frac{1}{a} \right)^2 + \left(\frac{1}{c} \right)^2 \right]^{-1/2} = 2.16 \text{ \AA}$ and

$$\frac{1}{2} \left[\left(\frac{1}{c} \right)^2 + \left(\frac{1}{b} \right)^2 \right]^{-1/2} = 2.30 \text{ \AA} \text{ respectively which need to be compared with the separation of the LSAT}$$

(111) planes of $\frac{a_o}{\sqrt{3}}=2.23$ Å thus leading to a 3% expansion and a 3% contraction, respectively, as given in Table I.

The two LSAT lattice vectors lying in plane are LSAT[1 $\bar{1}$ 0] and LSAT[11 $\bar{2}$] with lengths $\sqrt{2}a_0=5.47$ Å and $\sqrt{6}a_0=9.47$ Å respectively. The GMO lattice vectors are [010] and [10 $\bar{1}$] with lengths 5.84 Å and 9.13 Å respectively, relevant for the GMO(101) plane, and [100] and [01 $\bar{1}$] with lengths 5.31 Å and 9.13 Å respectively, relevant for GMO(011). The best fits for the GMO(101) plane are GMO[010] on LSAT[1 $\bar{1}$ 0] and GMO[01 $\bar{1}$] on LSAT[11 $\bar{2}$] and those for the GMO(011) plane are GMO[100] on LSAT[1 $\bar{1}$ 0] and GMO[01 $\bar{1}$] on LSAT[11 $\bar{2}$]. The strains, defined as $\frac{d_{LSAT} - d_{GMO}}{d_{GMO}} \times 100$, are given in Table I.

V. MAGNETISM

The magnetism of the films was studied and the results compared with those obtained for bulk GMO in order to investigate the effects of the epitaxy induced strain. In bulk there is a strongly temperature dependent paramagnetic response along both the b and c axes and hysteretic magnetisation occurs along the b axis [15].

We have measured field cooled (FC) and zero field cooled (ZFC) magnetisation in a field of 8×10^3 Am $^{-1}$ with the magnetic field in plane for the films as shown in Fig. 5(a) and (b). Hysteresis loops were measured at 5 K. The hysteresis loops showed two contributions, a part that varied linearly with the applied field at fields greater than 2×10^5 Am $^{-1}$ and a part that showed hysteresis; the data is shown in Figs. 5(c), (d), (e) and (f). The raw magnetic data from the LSAT substrates (shown in Section III) has been subtracted from the raw magnetic data for the film on the substrate in order to obtain all the data shown here.

The FC/ZFC results for the films are shown in Figs. 5(a) and (b). The FC/ZFC plots lie almost top of each other for all temperatures but for both films a larger difference appears between the FC and ZFC plots for temperatures less than ~ 25 K. The plots for the film on (100) show a clear transition at ~ 25 K however the transition is more rounded for the film on (111).

The inverse susceptibilities found from the ZFC plots, as illustrated in Figs. 6 (a) and (b), show two distinct regions in which a Curie law dependence is observed, these depend on the substrate. Above about 30K there is a paramagnetic contribution from Mn as well as Gd ions which is described by

Curie's law $\chi^{high} = \frac{C^{high}}{T + \theta^{high}}$ as seen in bulk samples, for a single crystal and a polycrystalline powder,

where the measured value of $p_{high}^2 = g_{Gd}^2 S_{Gd}(S_{Gd} + 1) + g_{Mn}^2 S_{Mn}(S_{Mn} + 1)$ was close to the free ion value of 87 [4, 21, 22]. There is a second region that is also well described by a Curie law for $8 < T < 30$ K,

where the Mn spins are canted but the Gd spins are still disordered, $\chi^{low} = \frac{C^{low}}{T + \theta^{low}}$, so that

$p_{low}^2 = g_{Gd}^2 S_{Gd}(S_{Gd} + 1) \cong 63$. This region is shown on an expanded scale in the inserts to Fig. 6.

The measured values of p_{eff}^2 and θ for the films, in high and low temperature regimes are given in Table II where it is seen that the observed values of p_{high}^2 measured in the high temperature range are close to those expected for free spins for the film on LSAT (100); however those for the film on LSAT(111) are systematically low. The values of θ_{high} found in the high temperature range for both films are close to ~ 50 K, larger than the 35 K observed in bulk material, this quantity is dependent on the competition between different interactions and hence is very sensitive to a change in the strain [19]. The ferromagnetic value of θ^{low} for the film on LSAT (100) corresponds to the ordering of the Gd spins that is observed in bulk at ~ 7 K. This appears to be occurring at a slightly higher temperature ~ 11 K (in our definition of θ in the Curie law a positive θ corresponds at antiferromagnetism and hence a ferromagnetic transition temperature T_C corresponds to a negative value of θ). Different behaviour is

seen for the film on LSAT (111) where θ^{low} is positive implying that the change in the interactions due to the strain causes the Gd spins to tend to order antiferromagnetically.

The different ordering of the films is seen clearly from the hysteresis loops found after subtraction of the signal from the substrate, shown in Fig 5 (c), (d), (e) and (f). Comparing the loops for the film on LSAT (100) the magnetisation and hysteresis are greater for the field in-plane. In bulk material the easy direction and the largest moment occur along the c -axis and this direction lies in plane for the dominant orientation [21]. The observed magnetisation at which the hysteresis disappears is 0.26 ($\mu_B/f.u.$) for this film is much lower than that observed for a single crystal, 3.75 ($\mu_B/f.u.$), at 5 K [15, 21, 23]. The coercive fields are $7.6 \times 10^4 \text{ Am}^{-1}$ and $3.2 \times 10^4 \text{ Am}^{-1}$ for fields parallel and perpendicular, respectively, which compare with the bulk value of $9.6 \times 10^4 \text{ Am}^{-1}$ [21, 22]. Hence the strain due to epitaxy on LSAT (100) has led to considerable reduction in the canted magnetisation. This implies that the strains that develop in bulk material as a result of the canting have been suppressed by the epitaxy with the substrate [14].

There is no hysteretic behaviour for the Gd ordering of the film on LSAT (111) which is consistent with the antiferromagnetic θ observed for this film. Hence the very considerable distortions described in Section IV have caused a qualitative change in the ordering of the Gd spins.

VI. OPTICAL ABSORPTION

The transmission spectra of blank LSAT (100) and (111) compared with that for GMO/LSAT (100) and LSAT (111) as shown in Fig.1 (b) have been used to obtain the absorption of the GMO films, as shown in Fig 7. The spectral range where LSAT is transparent has allowed us to make measurements over a larger spectral range up to 4.5 eV, as compared with 3.2 eV for STO.

The absorption spectrum of bulk GMO starts to appear with a small peak at the energy of 0.75 eV and rises approximately linearly to ~ 2.5 eV and then linearly again with an increased slope up to 3.5eV [7]. The absorption at higher energy is attributed to the charge transfer transition from O 2*p* to Mn 3*d*. The origin of the absorption peak observed for LaMnO₃ near 2 eV has been debated for a long time [2]. Recently, however, it has been shown convincingly that the 2 eV peak should be interpreted as an inter-site transition across the Mott gap [7]. The optical absorption for the films agrees with measurements on bulk GMO because the absorption rises approximately linearly with energy up to ~ 2.5 eV and then more rapidly at higher energies. The peak that is seen at ~ 2 eV due to an inter-site transition across the Mott gap in LaMnO₃ is suppressed in GMO due to distortions [7]. The absorption at energy above 3eV is attributed to the charge transfer transition from O 2*p* to Mn 3*d* [2, 4].

VII. MAGNETO-OPTICS

MCD measurements were taken for both blank substrates and films on the substrates in Faraday geometry using a photoelastic modulator [24, 25]. Results for GMO/LSAT (100) and LSAT (111) are shown in Fig. 8(a), where the contribution to the MCD of the substrate has been subtracted from the measured MCD of the film and the substrate. We find that the MCD for the two films are very similar in spite of the differences in their magnetic properties. The spectra have two features: first the peak at 2eV corresponding to the charge-transfer transition between the Mn d states split by the Jahn-Teller effect at ~ 2 eV and the change in slope at 3eV corresponding to the onset of the band edge transition from the oxygen p band to the d states at ~ 3 eV [2, 4-6]. It can be clearly seen that the MCD is much larger at 10K where the Mn spins are ordered. In Fig. 8(b) we compare the spectrum taken at 10K with that taken at 300K, scaled so the curves have similar magnitudes, in order to compare the spectral shapes. This indicates that the main effect is just a change in magnitude due to the magnetic ordering,

but that there is a small increase in the MCD magnitude between 2 eV and 3 eV, implying that the Jahn-Teller splitting has increased slightly at low temperatures.

VIII. CONCLUSIONS

The strain of the films due to the substrates causes substantial differences in the magnetic properties. The magnetic moment obtained in the range of 0.2 μB is due to the canted moments of Mn as the magnetic moment of Mn^{3+} is 4 μB . The canting of the Mn moments is enhanced and a strong easy plane anisotropy is induced by the strain caused by the LSAT (100) that is larger than that induced by STO(100); this is due to the extra compressive strain in plane along the b axis. The transition temperature is enhanced for the film grown on LSAT (100) to ~ 30 K which is higher than the value seen in bulk samples, 23K. The canted phase appears to be suppressed for the film grown on LSAT (111) and can be induced by a magnetic field of $2.0 \times 10^5 \text{ Am}^{-1}$. The Curie constant found by fitting the ZFC plot to a Curie law is also smaller for the films grown LSAT (111). The in-plane compression of the film grown on LSAT (100) causes a strong enhancement of the strength of the inter-site transition between Mn ions and a large enhancement of the MCD around 2 eV relative to the films grown on STO (100). In contrast the MCD is suppressed for the film grown on LSAT (111). Absorptions at lower energy originates from the Mn (3d) electrons transition, while the absorption at higher energy is associated with the charge-transfer transitions between O (2p) and Mn (3d) states. Using LSAT (100) and (111) allows us to make measurements over a larger spectral range above 3.25 eV compared to SrTiO_3 (100), because the STO is absorbing more strongly than the LSAT substrates for $E > 3.2$ eV. Large changes may be induced in GMO by growing thin epitaxial films on suitably chosen substrates. In particular a marked enhancement of the saturation magnetization and the coercive field may be obtained by growing on LSAT (100).

IX. Acknowledgments

We dedicate this article to the memory of our colleague Yakov Mukovskii who initiated this work but was unable to contribute to its development. The work was supported by a **Royal Society grant: International Exchanges 2012 RFBRIE120191** and the **Russian Academy of Science** by RFBR Grant 14-07-00258 **also** by studentships for M.S. Al Qahtani from King Saud University and for H Albargi from the Saudi Cultural Attaché.

X. REFERENCES

- [1] N. Andreev, V. Chichkov, T. Sviridova, N. Tabachkova, A. Volodin, C. Van Haesendonck, Y. Mukovskii, Growth, structure, surface topography and magnetic properties of GdMnO_3 multiferroic epitaxial thin films, EPJ Web of Conferences, 40 (2013) 15014.
- [2] W.S. Choi, S.J. Moon, S.S.A. Seo, D. Lee, J.H. Lee, P. Murugavel, T.W. Noh, Y.S. Lee, Optical spectroscopic investigation on the coupling of electronic and magnetic structure in multiferroic hexagonal RMnO_3 ($R=\text{Gd}$, Tb , Dy , and Ho) thin films, Physical Review B, 78 (2008) 054440.
- [3] X. Li, C. Lu, J. Dai, S. Dong, Y. Chen, N. Hu, G. Wu, M. Liu, Z. Yan, J.-M. Liu, Novel multiferroicity in GdMnO_3 thin films with self-assembled nano-twinned domains, Scientific Reports, 4 (2014) 7019.
- [4] S.A.Q. Mohammed, S.A. Marzook, H.J. Blythe, A.M. Fox, G.A. Gehring, N. Andreev, V. Chichkov, M. Ya, Magnetic and optical properties of multiferroic GdMnO_3 film, Journal of Physics: Conference Series, 391 (2012) 012083.
- [5] X.L. Wang, D. Li, T.Y. Cui, P. Kharel, W. Liu, Z.D. Zhang, Magnetic and optical properties of multiferroic GdMnO_3 nanoparticles, Journal of Applied Physics, 107 (2010) 09B510.
- [6] D.I. Khomskii, Multiferroics: Different ways to combine magnetism and ferroelectricity, Journal of Magnetism and Magnetic Materials, 306 (2006) 1-8.
- [7] M.W. Kim, S.J. Moon, J.H. Jung, J. Yu, S. Parashar, P. Murugavel, J.H. Lee, T.W. Noh, Effect of

- orbital rotation and mixing on the optical properties of orthorhombic $RMnO_3$ ($R=La, Pr, Nd, Gd$, and Tb), *Phys. Rev. Lett.*, 96 (2006) 247205.
- [8] J.B. Goodenough, Theory of The Role of Covalence in The Perovskite-Type Manganites [$La, M(II)$] MnO_3 , *Physical Review*, 100 (1955) 564-573.
- [9] J. Kanamori, Superexchange interaction and symmetry properties of electron orbitals, *journal of physics and chemistry of solids*, 10 (1959) 87-98.
- [10] D. Lee, J.H. Lee, P. Murugavel, S.Y. Jang, T.W. Noh, Y. Jo, M.H. Jung, Y.D. Ko, J.S. Chung, Epitaxial stabilization of artificial hexagonal $GdMnO_3$ thin films and their magnetic properties, *Applied Physics Letters*, . 90 (2007) 182540.
- [11] J.H. Lee, P. Murugavel, H. Ryu, D. Lee, J.Y. Jo, J.W. Kim, H.J. Kim, K.H. Kim, Y. Jo, M.H. Jung, Y.H. Oh, Y.W. Kim, J.G. Yoon, J.S. Chung, T.W. Noh, Epitaxial Stabilization of a New Multiferroic Hexagonal Phase of $TbMnO_3$ Thin Films, *Advanced Materials*, 18 (2006) 3125-3129.
- [12] B.H. Kim, B.I. Min, Nearest and next-nearest superexchange interactions in orthorhombic perovskite manganites $RMnO_3$ ($R=rare\ earth$), *Physical Review B*, 80 (2009) 064416.
- [13] T. Kimura, T. Goto, H. Shintani, K. Ishizaka, T. Arima, Y. Tokura, Magnetic control of ferroelectric polarization, *Nature*, 426 (2003) 55-58.
- [14] J. Baier, D. Meier, K. Berggold, J. Hemberger, A. Balbashov, J.A. Mydosh, T. Lorenz, Hysteresis effects in the phase diagram of multiferroic $GdMnO_3$, *Physical Review B*, 73 (2006) 100402.
- [15] T. Kimura, G. Lawes, T. Goto, Y. Tokura, A.P. Ramirez, Magnetoelectric phase diagrams of orthorhombic $RMnO_3$ ($R=Gd, Tb, and Dy$), *Physical Review B*, 71 (2005) 224425.
- [16] K. Noda, S. Nakamura, J. Nagayama, H. Kuwahara, Magnetic field and external-pressure effect on ferroelectricity in manganites: Comparison between $GdMnO_3$ and $TbMnO_3$, *Journal of Applied Physics*, 97 (2005) 103.
- [17] A.N. Timothy, W.-G. Travis, S. Zollner, Infrared and Visible Dielectric Properties of $(LaAlO_3)_{0.3}(Sr_2AlTaO_6)_{0.7}$, *Annual Meeting of the Four Corners Section of the APS Vol*, 58 (2013) No 12

- [18] B.-Q. Hu, X.-M. Wang, T. Zhou, Z.-Y. Zhao, X. Wu, X.-L. Chen, Transmittance and Refractive Index of the Lanthanum Strontium Aluminium Tantalum Oxide Crystal, Chinese Physics Letters, 18 (2001) 278.
- [19] J.M.D. Coey, Dilute magnetic oxides, Current Opinion in Solid State and Materials Science, 10 (2006) 83-92.
- [20] X. Marti, F. Sanchez, V. Skumryev, V. Laukhin, C. Ferrater, M.V. Garcia-Cuenca, M. Varela, J. Fontcuberta, Crystal texture selection in epitaxies of orthorhombic antiferromagnetic YMnO_3 films, Thin Solid Films, 516 (2008) 4899-4907.
- [21] J. Hemberger, S. Lobina, H.A. Krug von Nidda, N. Tristan, V.Y. Ivanov, A.A. Mukhin, A.M. Balbashov, A. Loidl, Complex interplay of $3d$ and $4f$ magnetism in $\text{La}_{1-x}\text{Gd}_x\text{MnO}_3$, Physical Review B, 70 (2004) 024414.
- [22] P. Negi, G. Dixit, H.M. Agrawal, R.C. Srivastava, Structural, Optical and Magnetic Properties of Multiferroic GdMnO_3 Nanoparticles, Journal of Superconductivity and Novel Magnetism, 26 (2013) 1611-1615.
- [23] M.W. Kim, P. Murugavel, P. Sachin, J.S. Lee, T.W. Noh, Origin of the 2 eV peak in optical absorption spectra of LaMnO_3 : an explanation based on the orbitally degenerate Hubbard model, New Journal of Physics, 6 (2004) 156.
- [24] S. Katsuaki, Measurement of Magneto-Optical Kerr Effect Using Piezo-Birefringent Modulator, Japanese Journal of Applied Physics, 20 (1981) 2403.
- [25] W.P. Van Drent, T. Suzuki, Ultra-violet range magneto-optic study of FCC-Co and Co/Pt multilayers, Journal of Magnetism and Magnetic Materials, 175 (1997) 53-62.

Figures Captions

FIG. 1: Fig. 1: The transmission spectra (a) for blank LSAT (100) and (111) and (b) after the deposition of GMO films on the substrates.

FIG. 2: Magnetic properties of blank LSAT (100) and LSAT (111) substrates. FC/ZFC cooled measurements with the applied magnetic field, $8 \times 10^{-3} \text{ Am}^{-1}$, lying in plane. Hysteresis loops taken at 300K in (c) and (d); equivalent hysteresis loops taken at 5K in (e) and (f).

FIG. 3: (a) Part of the symmetrical spectrum using $\text{CoK}\alpha$ radiation (b) Pole figure for (111) film reflection, $2\theta=30^\circ$, (c) β -scan $\psi = 45$, $2\theta=38.3^\circ$, LSAT (011) (d) β -scan $\psi=62$, $2\theta=30.0^\circ$, GdMnO_3 (111) and (e) β -scan $\psi=28$, $2\theta=29.94^\circ$, GdMnO_3 (111).

FIG. 4: Symmetrical spectra of LSAT and $\text{GdMnO}_3/\text{LSAT}$ (111) where the peak has been blown up at $\sim 40^\circ$.

FIG. 5: (a) The FC and ZFC plots taken in an in-plane field of $H = 8.0 \times 10^3 \text{ Am}^{-1}$ for the GMO film on (a) LSAT (100) and (b) LSAT (111); Magnetic hysteresis loops of the film taken at 5K with the applied magnetic field in both parallel and perpendicular directions for the film on (c) and (d) on LSAT (100) and (e) and (f) on LSAT(111). In all cases the magnetic contribution from the substrate has been subtracted as shown in these figures.

FIG. 6: (a) The inverse susceptibility obtained from ZFC measurements of GMO/LSAT (100) and (b) GMO / LSAT (111), where the magnetic field was applied in-plane; the contributions from the substrates have been subtracted, the insets in (a) and (b) show the low temperature regions; (c) the inverse susceptibility of the film of GMO /STO (100).

FIG. 7: Absorption measurements of $\text{GdMnO}_3/\text{LSAT}$ (100) and $\text{GdMnO}_3/\text{LSAT}$ (111) in $1.75 < E < 3.5$, the inset shows the absorption in $3.5 < E < 4.5$.

FIG. 8: (a) MCD spectra of $\text{GdMnO}_3/\text{LSAT}$ (100) and $\text{GdMnO}_3/\text{LSAT}$ (111) at 10 K and 300 K, (b) MCD spectra of $\text{GdMnO}_3/\text{LSAT}$ (100) and $\text{GdMnO}_3/\text{LSAT}$ (111) at 10 K and 300 K where 300K has been blown up, the effects of substrates have been subtracted.

Tables of Captions

1. **Table I:** The separations between planes and the strains induced along the axes perpendicular to the planes by the epitaxial growth modes for GMO on LSAT (100) and LSAT (111).
2. **Table II:** The calculated and measured Curie constants of $\text{GdMnO}_3/\text{LSAT}$ (100) and LSAT (111).

Table I: The separations between planes and the strains induced along the axes perpendicular to the planes by the epitaxial growth modes for GMO on LSAT (100) and LSAT (111).

	Spacing	Misfit between planes	In plane misfit	In plane misfit
GMO plane on LSAT (100)				
(110)	$\left[\left(\frac{1}{a}\right)^2 + \left(\frac{1}{b}\right)^2\right]^{-1/2}$	-1.5%	GMO[001] on LSAT[0 $\bar{2}$ 0] 5%	GMO[1 $\bar{1}$ 0] on LSAT[00 $\bar{2}$] - 2%
(001)	c	5%	GMO[0 $\bar{2}$ 0] on LSAT[0 $\bar{3}$ 0] -0.6%	GMO[$\bar{3}$ 00] on 4LSAT[00 $\bar{4}$] -3%
GMO Plane on LSAT (111)				
(101)	$\left[\left(\frac{1}{a}\right)^2 + \left(\frac{1}{c}\right)^2\right]^{-1/2}$	3%	GMO[010] on LSAT[1 $\bar{1}$ 0] -6%	GMO[10 $\bar{1}$] on LSAT[11 $\bar{2}$] 4%
(011)	$\left[\left(\frac{1}{b}\right)^2 + \left(\frac{1}{c}\right)^2\right]^{-1/2}$	-3%	GMO[100] on LSAT[1 $\bar{1}$ 0] 3%	GMO[01 $\bar{1}$] on LSAT[11 $\bar{2}$] 0.3%

Table II: The measured effective moments and Weiss constants of GMO/LSAT (100), LSAT (111) and STO (100) in the high and low temperature regimes.

Sample	GMO/LSAT(100)	GMO/LSAT(111)	GMO/STO(100)
p_{high}^2	84±5	71±7	76±10
p_{low}^2	68±7	52±10	45±10
θ_{high}	42 ± 5	47 ± 5	43±5
θ_{low}	-12 ± 2	6± 2	8± 2

Fig. 1a

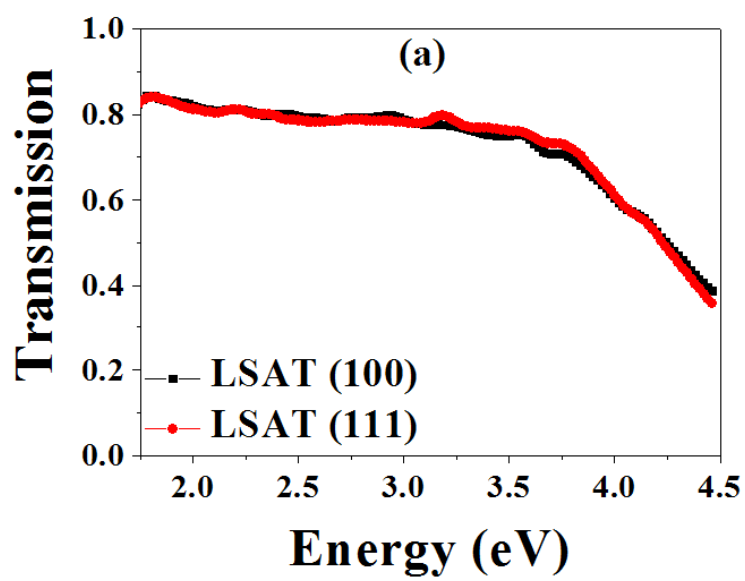


Fig. 1b

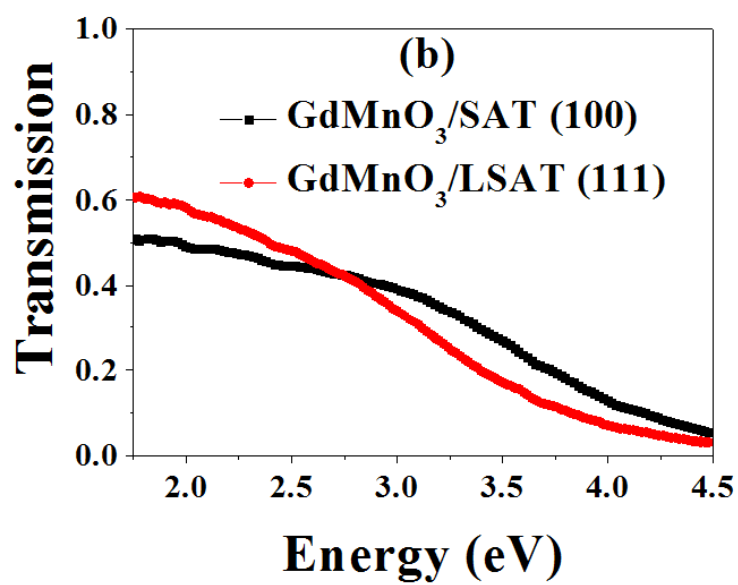


Fig. 2a

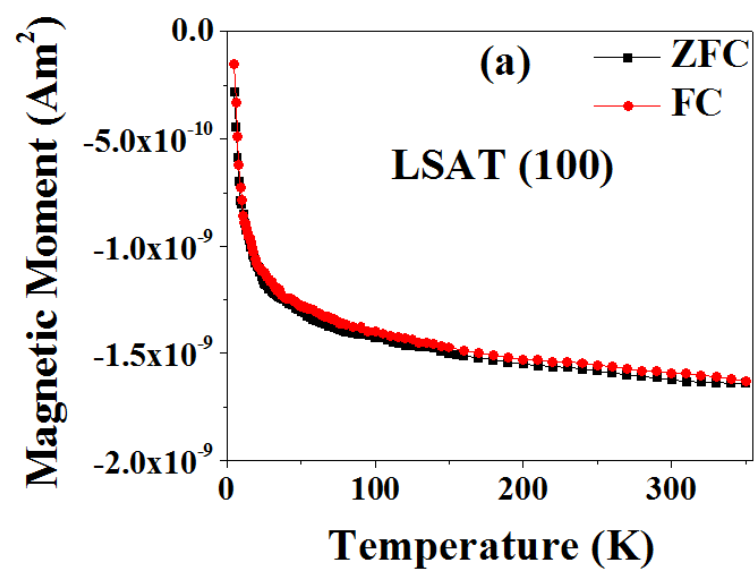


Fig. 2b

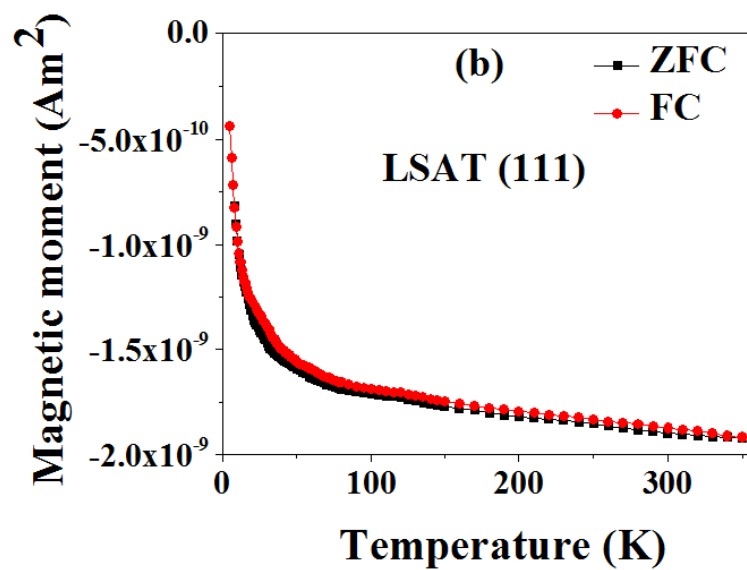


Fig. 2c

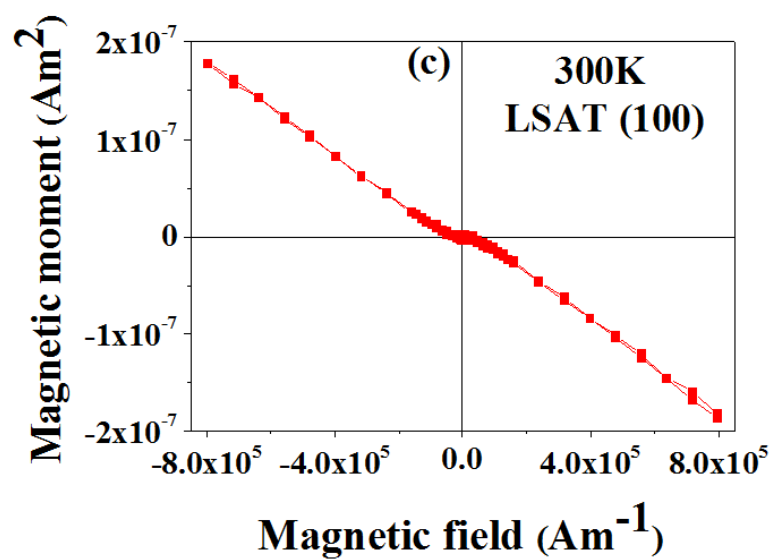


Fig. 2d

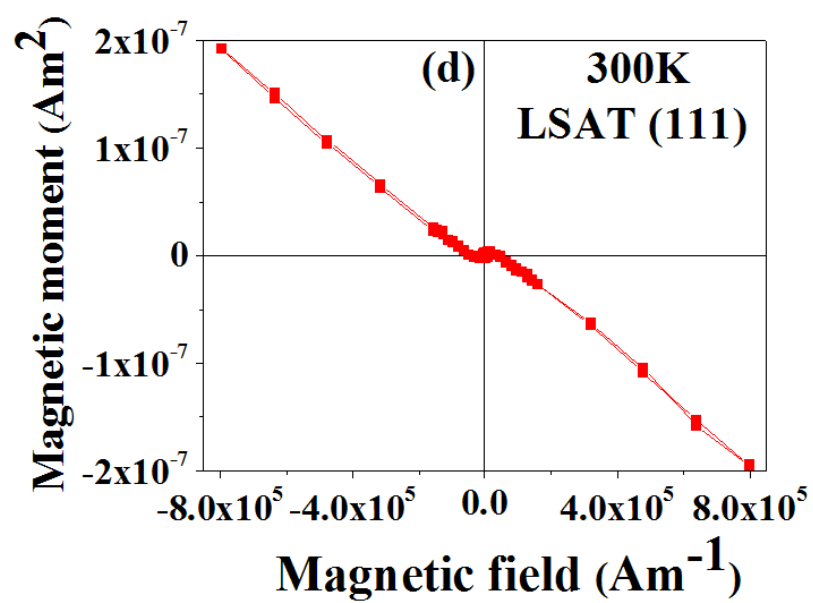


Fig. 2e

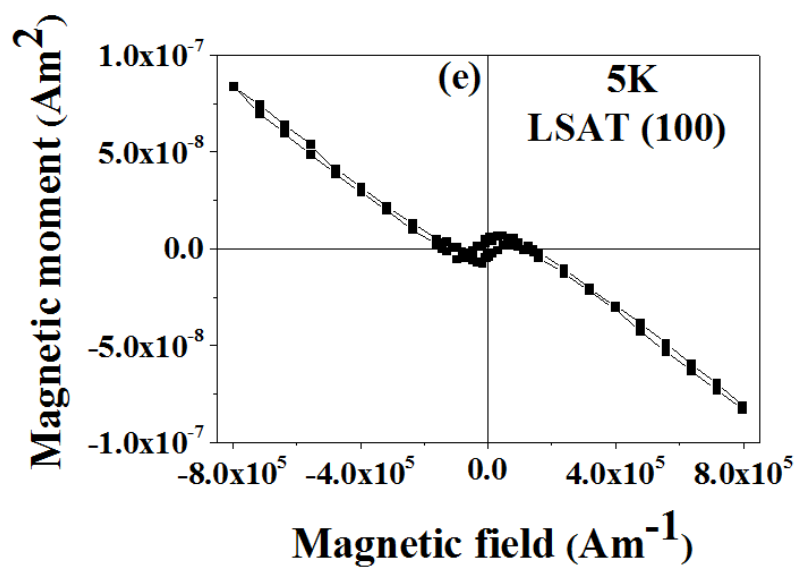


Fig. 2f

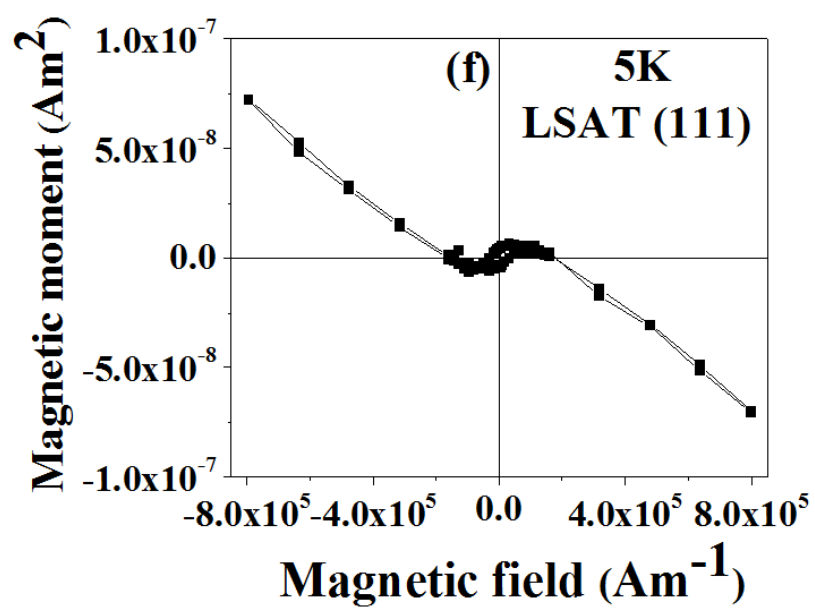


Fig. 3a

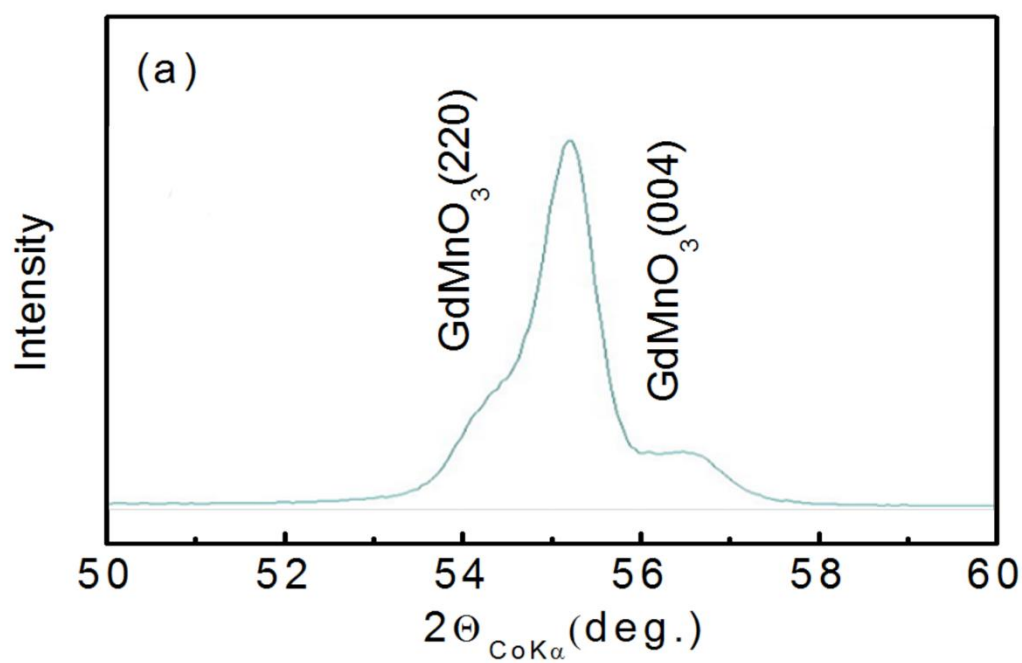


Fig. 3b

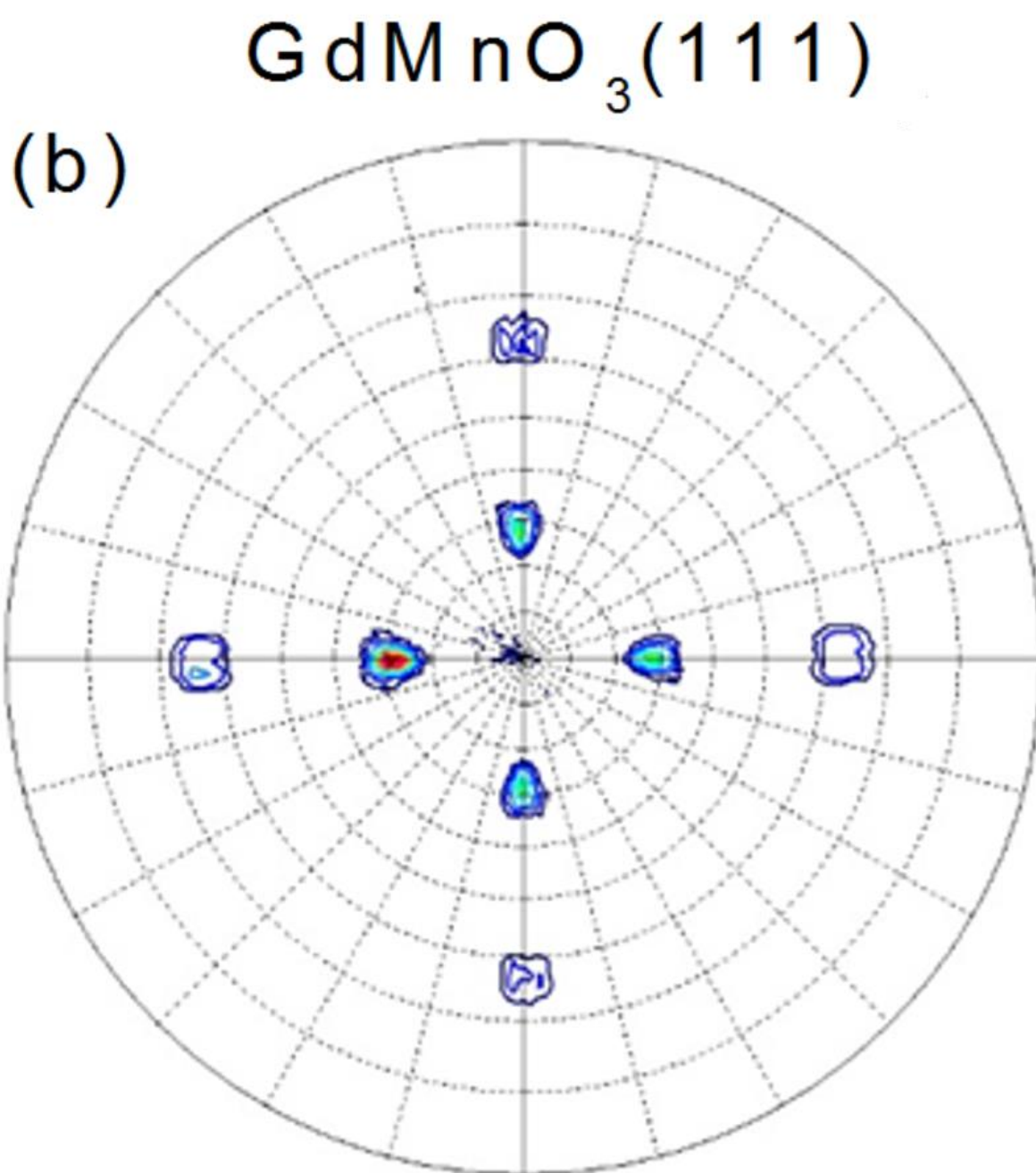


Fig. 3c

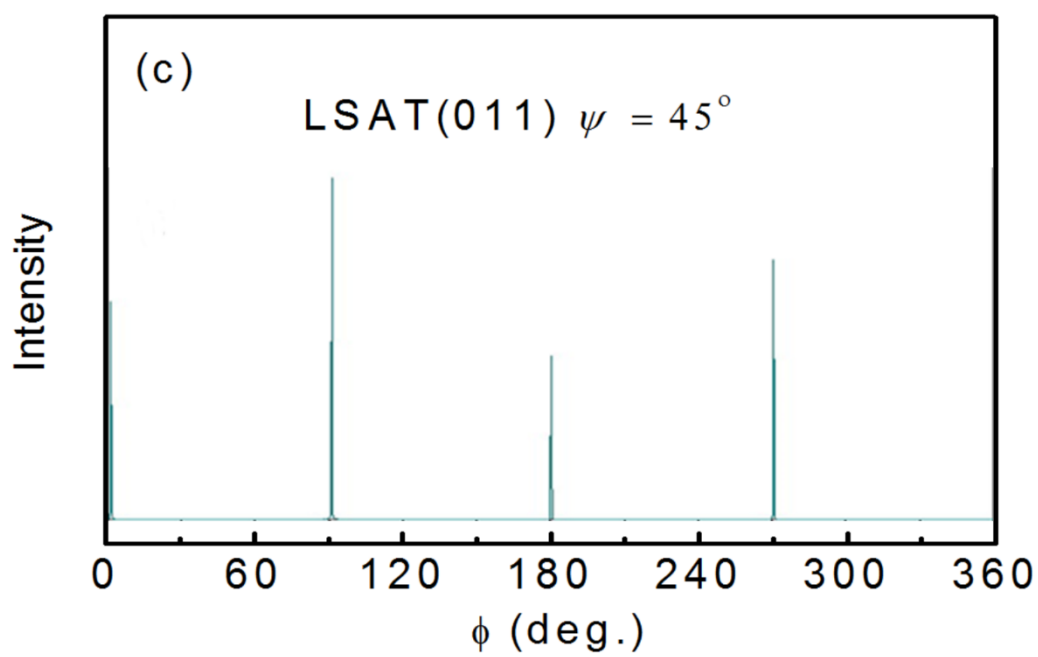


Fig. 3d

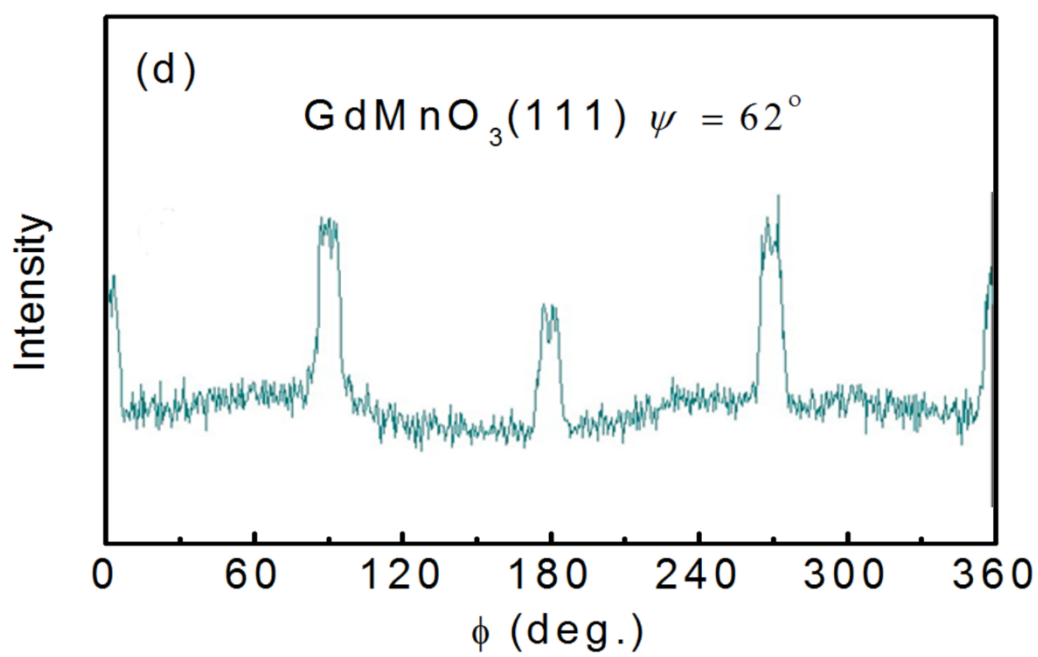


Fig. 3e

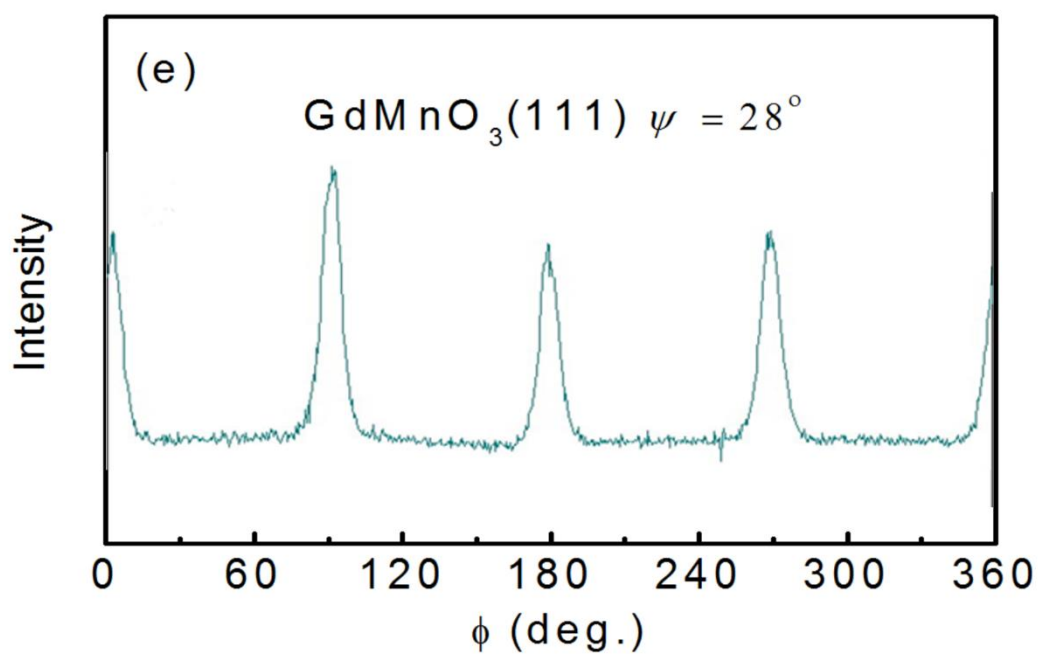


Fig. 4

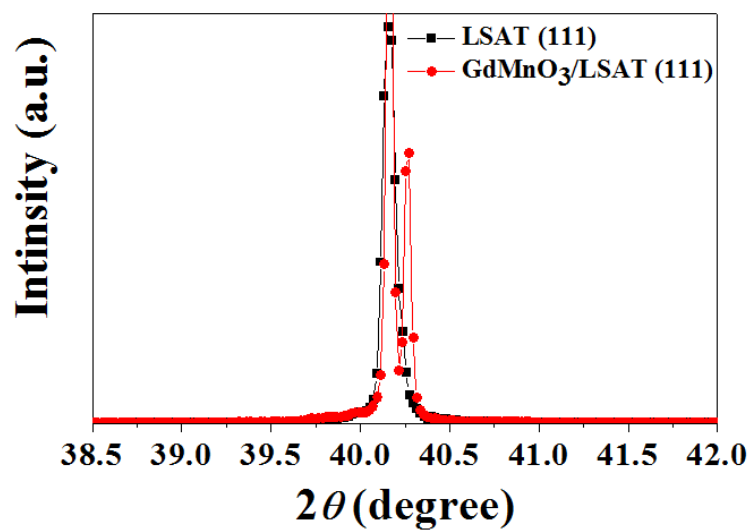


Fig. 5a

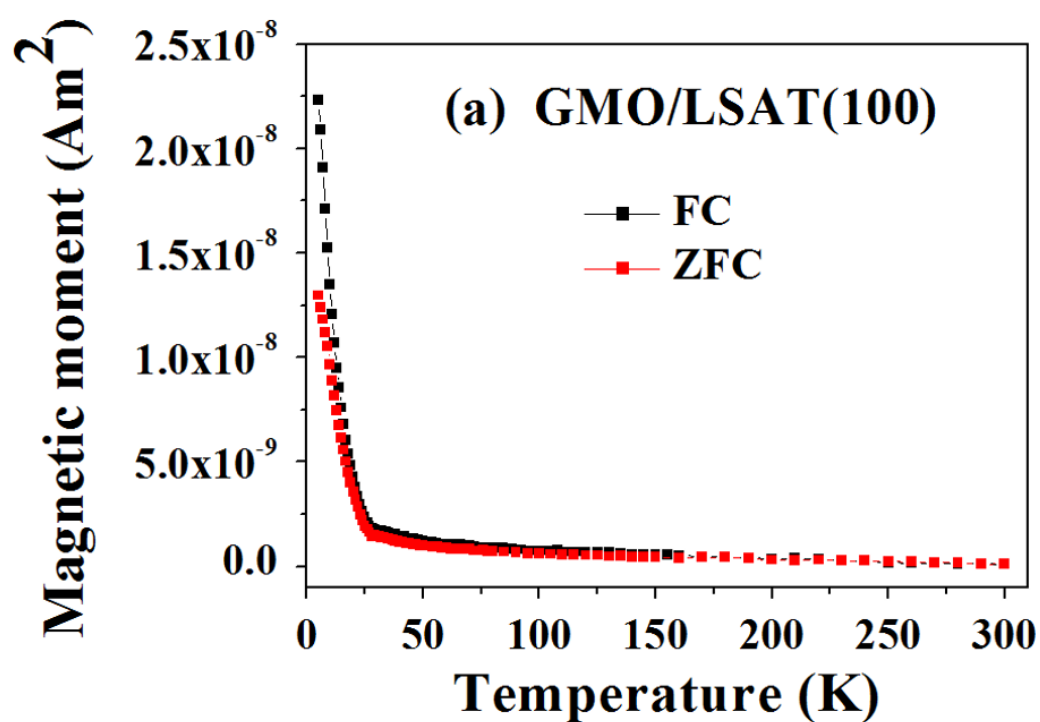


Fig. 5b

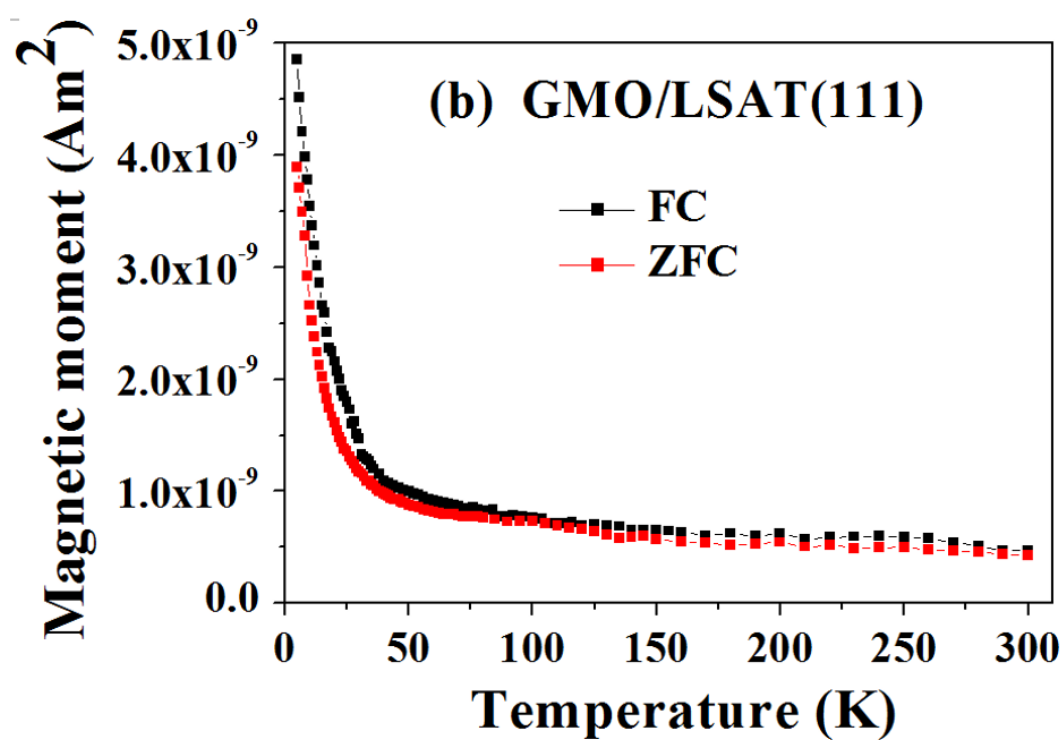


Fig. 5c

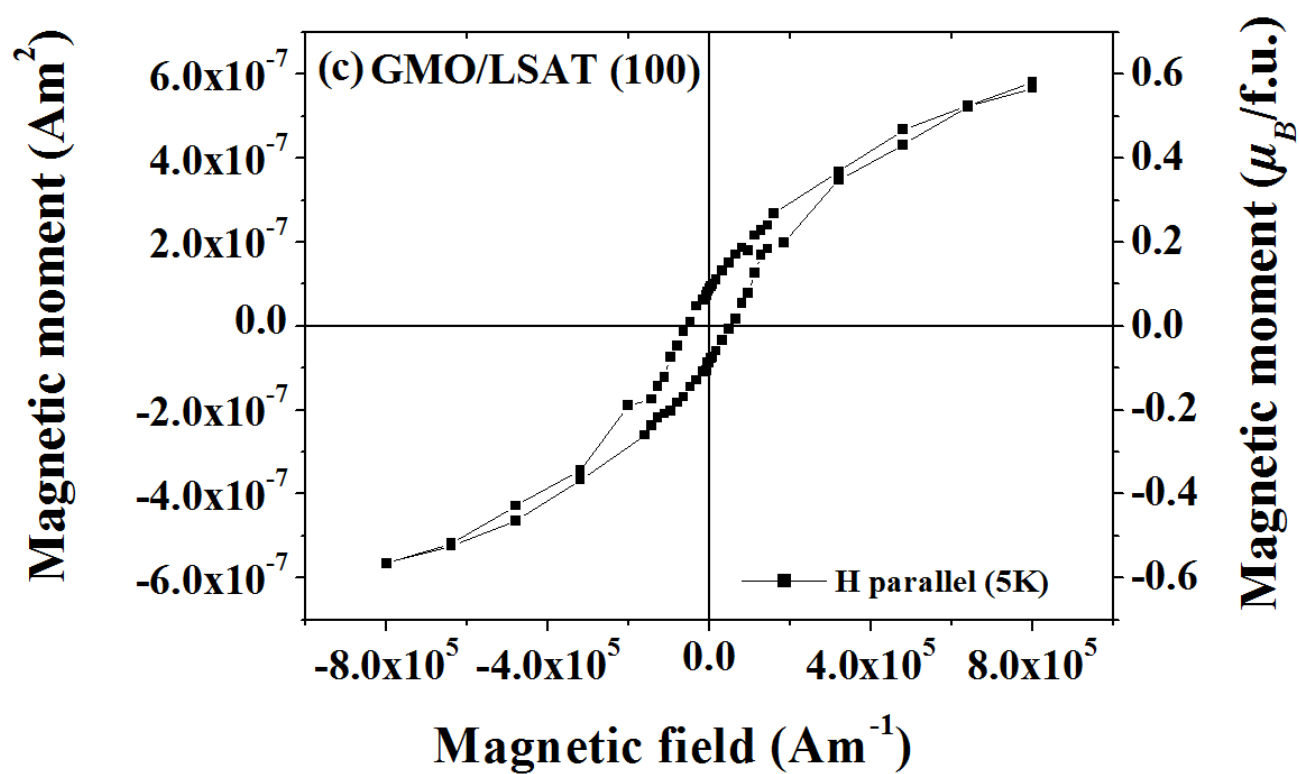


Fig. 5d

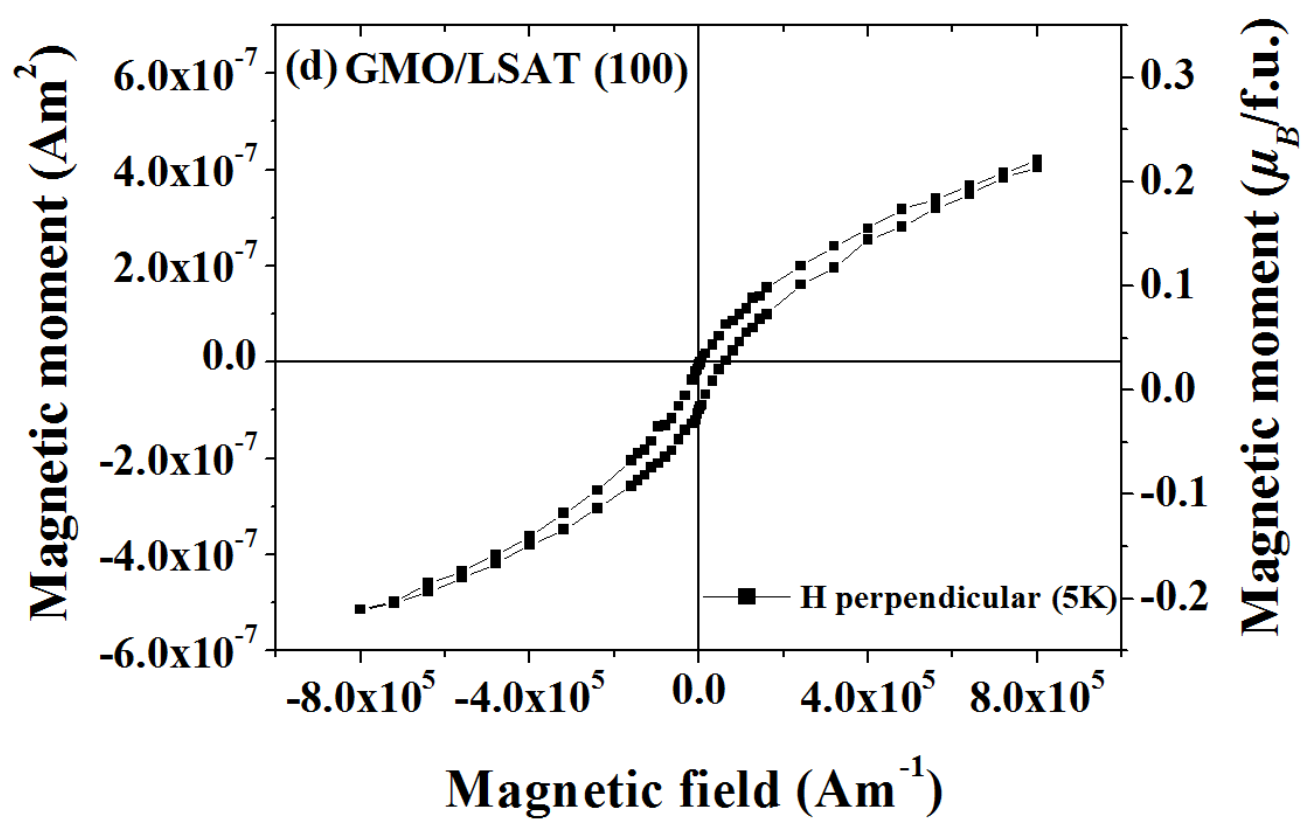


Fig. 5e

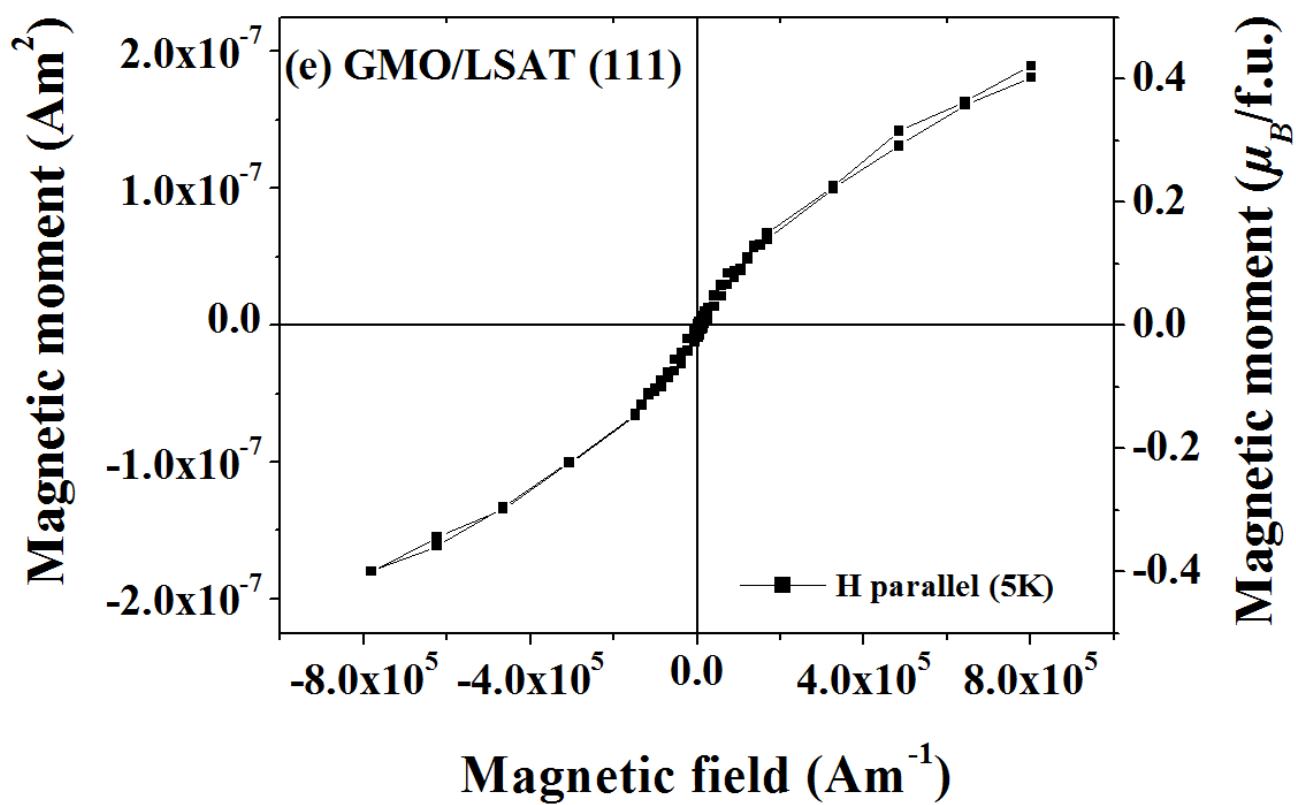


Fig. 5f

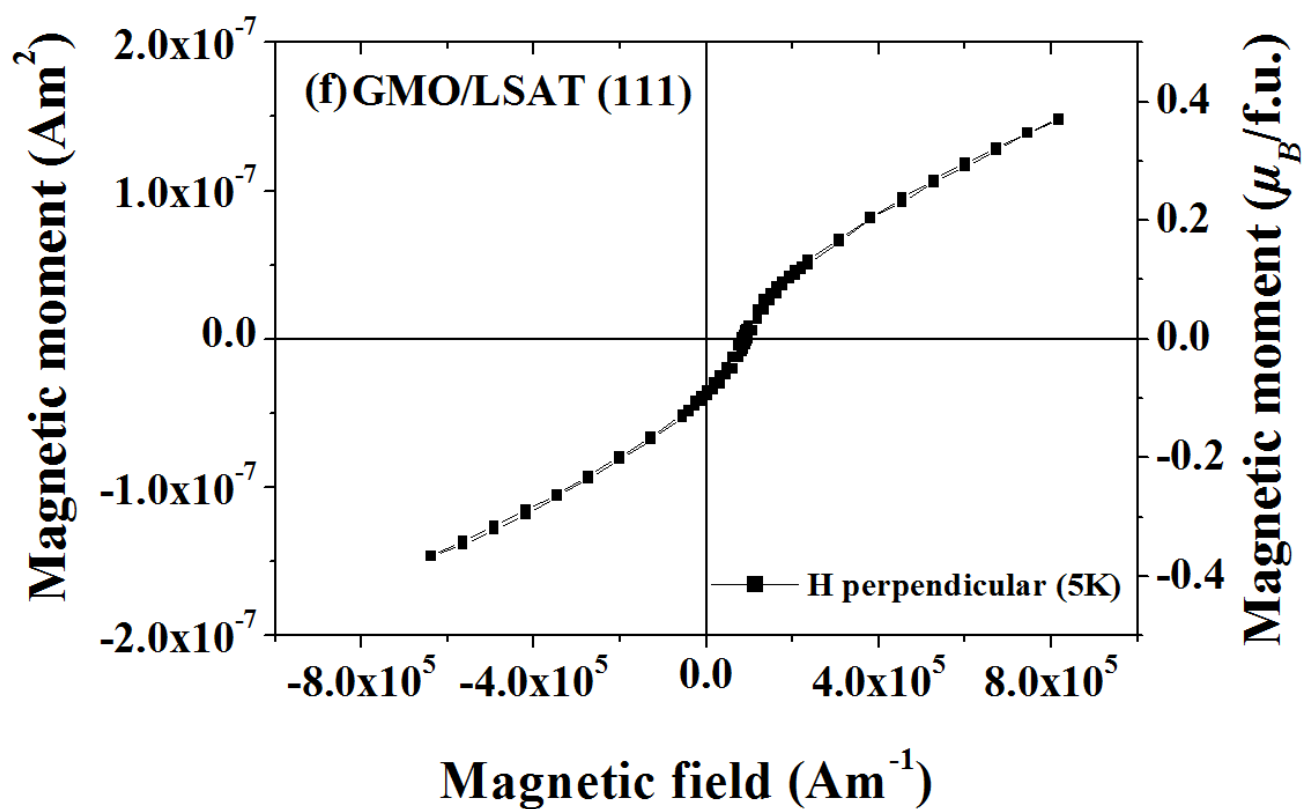


Fig. 6a

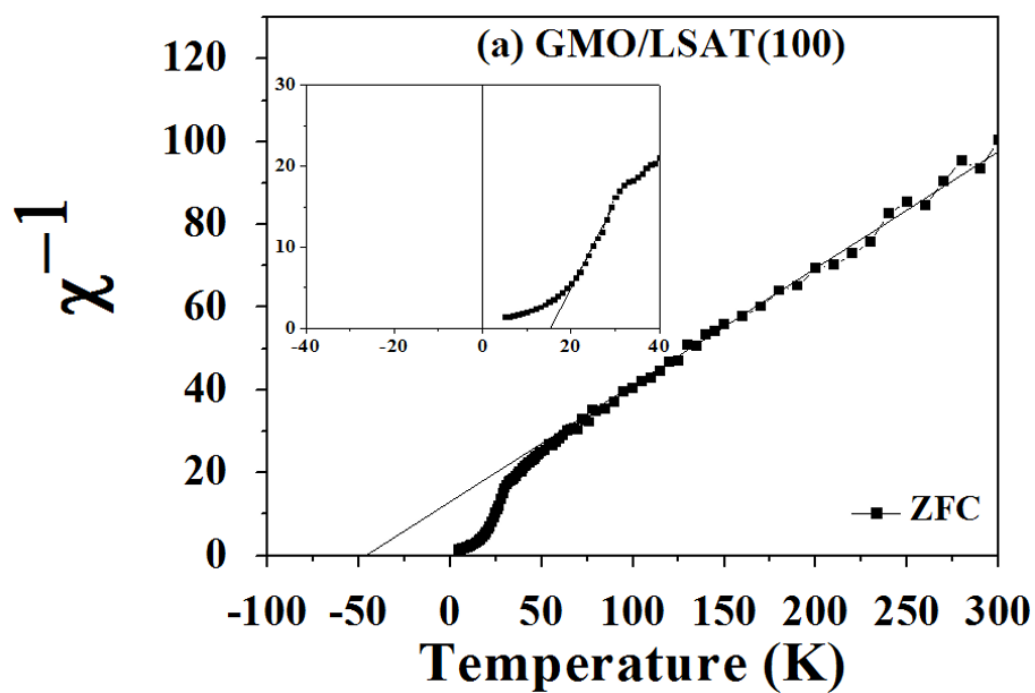


Fig. 6b

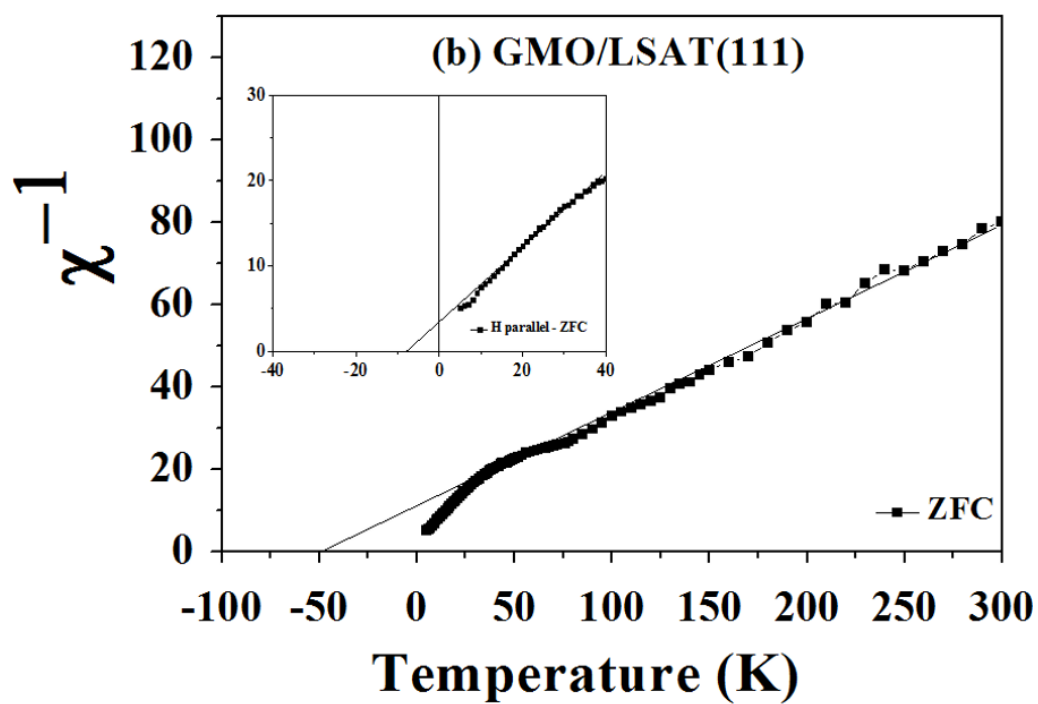


Fig. 6c

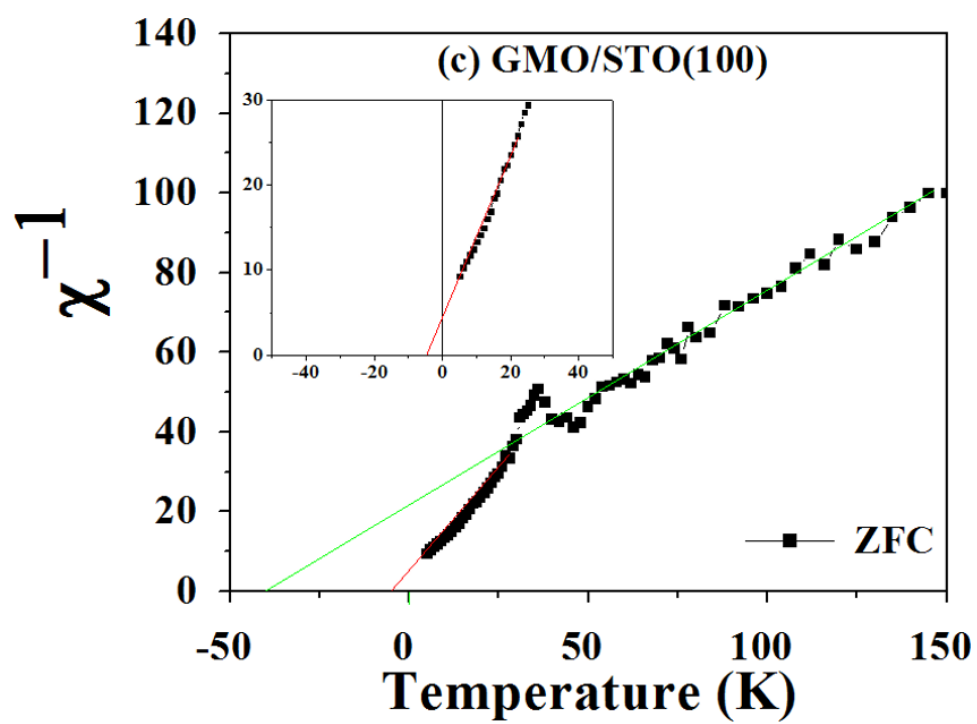


Fig. 7

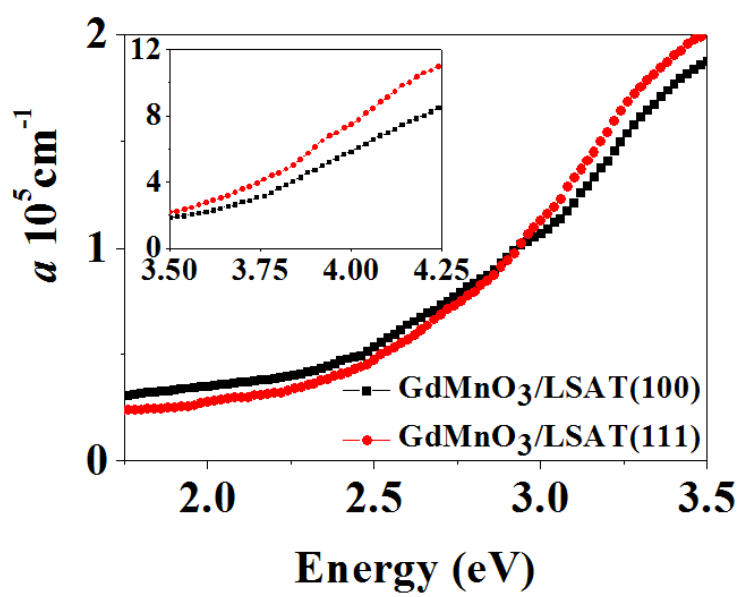


Fig. 8a

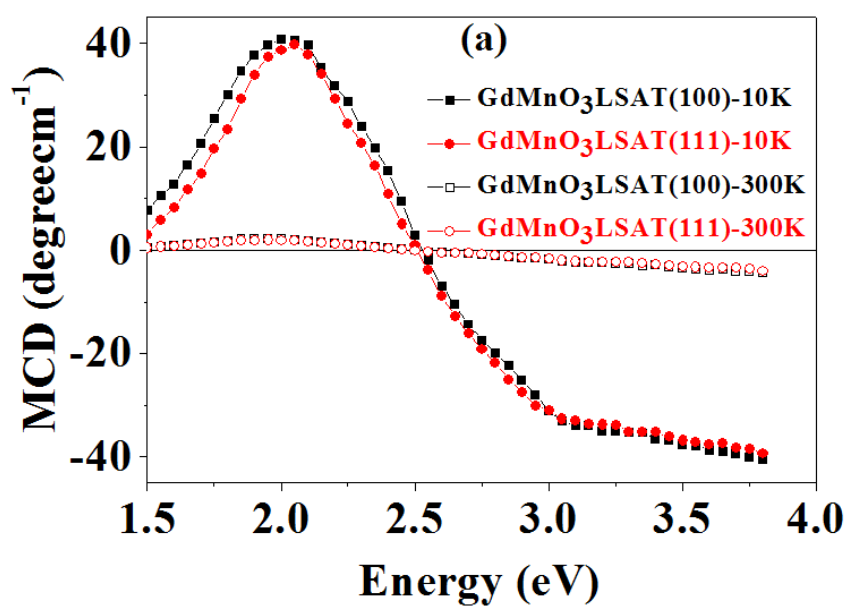
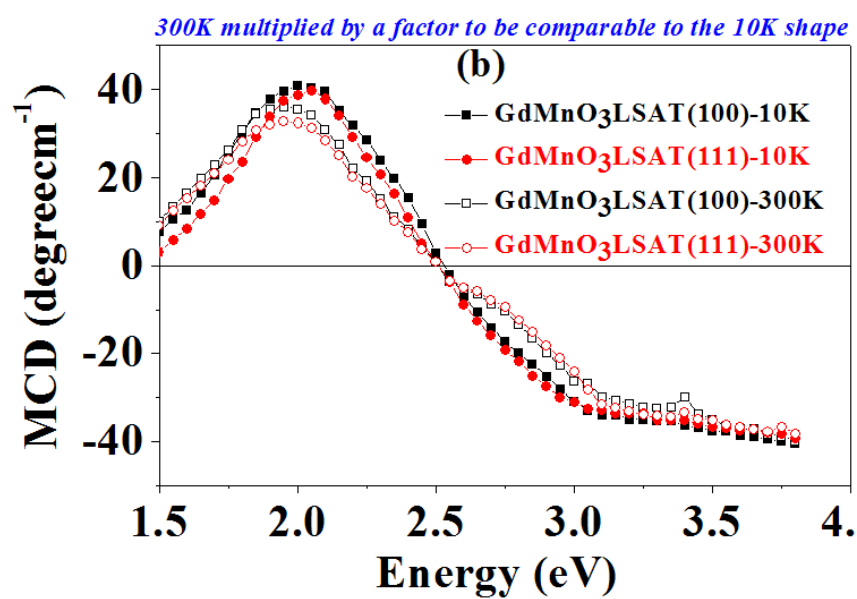


Fig. 8b



Research Highlights

- GdMnO_3 (GMO) films grown on different $(\text{LaAlO}_3)_{0.3}(\text{Sr}_2\text{AlTaO}_6)_{0.7}$ (LSAT) substrates.
- GMO/LSAT films have been compared to GMO grown on SrTiO_3 (STO) substrate.
- Strain can be introduced in GMO films by different orientations of LSAT substrates.
- Different properties of GMO/LSAT have been found to be highly dependent on strain.
- Optical properties of GMO/LSAT can be measured over a larger spectral range than GMO/STO.